

SEISMIC BEHAVIOR OF DAMAGED BUILDINGS: A COMPARISON OF STATIC AND DYNAMIC NONLINEAR APPROACH

Maria Polese¹, Marco Gaetani d'Aragona¹, Andrea Prota¹ and Gaetano Manfredi¹

¹ Department of Structures for Engineering and Architecture, University of Naples Federico II
via Claudio 21, 80125 Naples, Italy

e-mail: maria.polese@unina.it; marco.gaetanidaragona@unina.it; andrea.prota@unina.it;
gaetano.manfredi@unina.it

Keywords: residual capacity, damaged building, pushover analysis, nonlinear time history analysis, post-earthquake assessment, reinforced concrete frame.

Abstract. *Seismic behavior of damaged buildings may be expressed as a function of their Residual Capacity (REC_{ag}), that is a measure of seismic capacity “reduced” due to damage and represented in terms of peak ground acceleration a_g . REC_{ag} may be estimated through pushover analyses. In fact, adopting a lumped plasticity model, the plastic hinges may be suitably modified to account for the damage level of the single elements [1]; as shown in [2] nonlinear static analyses of the modified damaged models yield pushover curves that, depending on the number of elements involved in the damaged mechanism and on their damage level, may differ significantly with respect to original ones. The applicability of Pushover Analyses (PA) has been demonstrated for regular structures [3, 4], with their significance being generally supported by the comparison of the results obtained by these “simplified” analyses with Nonlinear dynamic Time-History (NTH) analyses. However, the usability of pushover analysis for the assessment of the behavior of damaged buildings has not been verified yet, and the study presented in this paper aims at contributing in the evaluation of this issue. The results of PA are confronted with those of NTH for Multi Degree Of Freedom (MDOF) systems representative of existing R.C. building typologies in the Mediterranean regions. In particular, the response (and damage) of each one of the original “intact” MDOF systems for earthquakes of increasing intensity is studied with either the PA and NTH. Next, applying the methodology described in [2], damage dependent behavior is estimated for varying levels of initial seismic (damaging) intensity. The maximum inter-storey drift and shape along the height, as well as the “modified” REC_{ag} are compared to the ones that could be obtained with NTH by subsequent application of suitably scaled pairs of accelerograms. The results of this study suggest that degree of approximation that is obtained by PA applied to damaged structures with respect to NTH does not vary with respect to the approximation of standard PA compared to NTH.*

1 INTRODUCTION

Seismic behavior of damaged buildings, and their relative seismic safety, may be suitably represented by their seismic capacity modified due to damage, the so-called REsidual Capacity (*REC*). Indeed, in the guidelines for seismic assessment of damaged buildings [5], the building tagging is based on the likelihood that an aftershock will exceed a specific (reduced) capacity associated with each damage state representing the quantitative measure of degradation. In [2] *REC* is defined as a parameter aimed at representing the building seismic capacity (up to collapse) in terms of a spectral quantity; in particular, REC_{Sa} of a building is defined as the smallest ground motion spectral acceleration (at period T_{eq} of the Single Degree Of Freedom SDOF system equivalent to the real structure) corresponding to collapse state of the building. Considering the seismic demand and the local damage that the elements in a Multi Degree of Freedom (MDOF) system may be forced to sustain due to a mainshock earthquake, the system's capacity may be considerably reduced, as evidenced in [2]. Because of the convenience of direct estimation of peak ground acceleration, a_g , as a damaging intensity parameter, the residual capacity is evaluated also in terms of a_g : given the spectral shape, REC_{ag} is the minimum anchoring peak ground acceleration such as to determine building collapse and corresponds to REC_{Sa} scaled by the spectral amplification factor for T_{eq} . By way of example, with reference to an EC8 spectral shape [6] and considering a system with $T_C < T_{eq} < T_D$, the following relation applies:

$$REC_{ag} = \frac{REC_{Sa}}{(S \cdot \eta \cdot 2.5)} \cdot \left(\frac{T_{eq}}{T_C} \right) \quad (1)$$

As explained in [2], and briefly summarized in [7], *REC* (REC_{Sa} and/or REC_{ag}) may be evaluated based on Pushover Analyses (PA) obtained for the structure in different (initial) damage state configurations, where the behavior of the damaged building is simulated with modification of plastic hinges for damaged elements. Ideally, Nonlinear dynamic Time-History (NTH) analyses, that predicts the forces and cumulative deformation (damage) demands in every element of the structural system, would be the best solution for capturing building's seismic performance. In fact, the use of structural models with appropriate stiffness/strength deterioration mechanisms would allow the simulation of response taking into account the cyclic accumulation of damage. However, NTH is a quite complex and time consuming analysis, hardly suitable for practical design/assessment by engineering professionals. In addition, in order to overcome the sensitivity of dynamic response to the characteristics of the input motions, a suite of representative accelerograms has to be carefully selected, greatly increasing the computational effort.

For the above reasons, it was preferred to rely on pushover based procedure for the assessment of the behavior of damaged buildings. PA represent an optimal compromise between the need to investigate building's nonlinear behavior and to perform a relatively simple static analysis, applicable for design/assessment purposes by practitioners. Indeed, under the limitation of applying it mainly to building structures oscillating predominantly in a single (fundamental) mode, standard PA allows a sound evaluation of damage progression for increasing levels of seismic demand and investigation of damage distribution within the MDOF systems [8].

The applicability of PA has been evaluated in several previous studies [3, 4, 9-12]. The first studies followed the approach of comparing the results of PA with those of NTH only at

certain loading levels, e.g. design level, or at equal top displacement (roof displacement from pushover equal to the maximum dynamic roof displacement). For example, in [10, 11] a set of 10 and 7 ground motions, respectively, were selected so to be compatible with given spectral shapes, and comparison of PA results with those of NTH analyses were performed, for a single scaling of those ground motions, in terms of displacements (or deflection profiles), inter-storey drifts and plastic hinge rotations. More recently, [4, 12] presented more exhaustive comparisons, developing complete pushover-like load–displacement curves from incremental dynamic analysis up to collapse for different structural configurations. They compared the pushover curves obtained for different lateral load distributions with the dynamic envelopes (maximum absolute drifts and base shear) obtained for increasing levels of ground motion intensity.

Despite the availability of several validation examples for PA, the usability of pushover analysis for the assessment of the behavior of damaged buildings [2] has not been verified yet, and the study presented in this paper aims at contributing in the evaluation of this issue.

Two MDOF frame systems, representative of mid and high rise existing RC buildings in the Mediterranean region, are analyzed and results obtained with pushover based procedure and NTH compared.

Section 2 of this paper presents the geometry and nonlinear (static and dynamic) modeling of the two studied frames, also explaining the use of plastic hinge modification factors for PA of damaged building.

Adopting REC_0 ($REC_{Sa,0}$ and/or $REC_{ag,0}$) and REC_i ($REC_{Sa,i}$ and/or $REC_{ag,i}$) as representative parameter for the seismic capacity of a building in its intact and generic i^{th} damaged state, we follow the approach of comparing the REC that can be obtained via PA with the one that may be evaluated via NTH. In addition, also the lateral maximum inter-storey drift profiles are compared.

Section 3 describes the assessment of REC_0 and REC_i with the pushover based approach. In particular, REC_0 is evaluated with PA adopting a lumped plasticity model. Next, as described in [2], based on the damage level D_i that is attained due to an hypothetical main-shock, the inelastic model is modified and PA re-executed, so that REC_i can be obtained.

Next, section 4 describes the evaluation via NTH analysis, with PA-NTH comparisons being presented and discussed in section 5.

2 DESCRIPTION OF THE BUILDING AND MODELING ASSUMPTIONS

The comparison of PA with NTH analysis is performed with reference to two bare Reinforced Concrete Frames (RCF), of 4 and 8 storeys respectively (see Figure 1), that have been designed to be representative of existing under-designed buildings in the Mediterranean area. In particular, the RCF were designed with a simulated design procedure as suggested in [13] and in the first seismicity class with reference to old seismic codes [14] in force in the beginning of age '60s, not applying principles of capacity design or proper reinforcement detailing and based on allowable stress method. The structure of the RCFs, that represent the perimeter frames of buildings with planar dimensions of 18m x10m, is formed by two bays of 5 m length, while the inter-storey height is of 3 m. As explained in [7], the simulated design is performed with allowable stresses for concrete of $\sigma_c = 6$ MPa for columns and 7.5 MPa for beams, while the allowable stress for steel, that considering the design period is assumed to be a smooth type Aq50 [14], is $\sigma_s = 180$ MPa [15].

The columns dimensions are represented in Figure 1. For what concern the beams, their dimension for the 4 storey RCF vary from 30x60 at the first two storeys to 30x50 at the upper ones, while for 8 storey building the beams at the first three storeys have section 35x65, 30x60 at fifth and sixth storeys, and 30x50 at the upper ones.

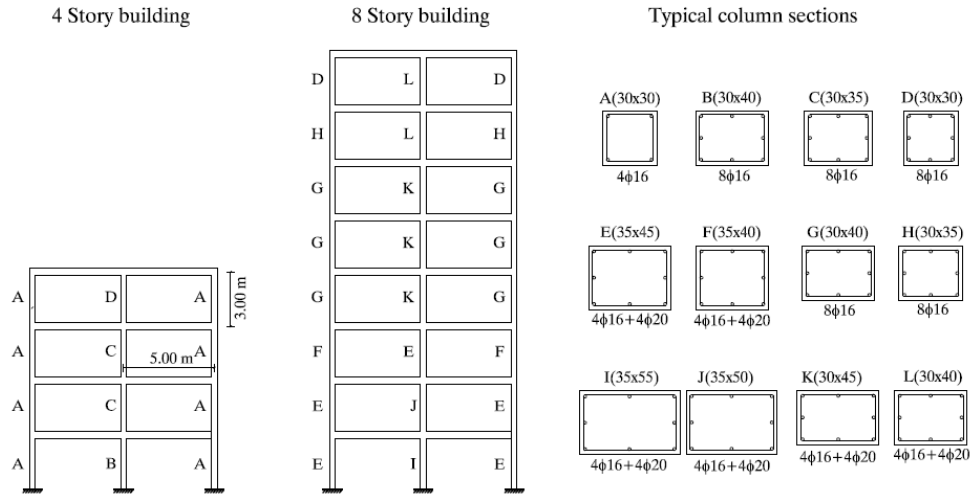


Figure 1: Model geometry and typical columns section and reinforcement.

2.1 Modeling issues for Pushover Analysis

Structural modeling, numerical analyses and post-processing of damage data, including the 3D graphic visualization of the deformed shape, are performed through the “PBEE toolbox” [16], which allows rapid generation of simple nonlinear models and the analysis of RC frames combining MATLAB® with OpenSees [17]. The toolbox was suitably modified in order to allow definition of bilinear plastic hinges according to ASCE-SEI/41 [18] and in order to allow the plastic hinge modification for the analyses of damaged buildings, as described later.

A lumped plasticity model was adopted for the two-dimensional MDOF Reinforced Concrete Frame buildings. The model is very simplified, not including geometric nonlinearity (i.e. $P-\Delta$ effects). In addition, although brittle shear failures in columns or beams may be expected in existing under-designed buildings [19, 20] and brittle behavior of beam-columns joints [21] is an additional vulnerability factor, these aspects are not considered in this study. Indeed, the main aim of this study is to test the capability of PA to capture, after suitable modification of flexural type plastic hinges, the post-seismic behavior of a damaged building. Therefore, in order to avoid introducing further complexity in the model the sole flexural behavior is explicitly investigated.

For RCF buildings, element flexural behavior is conveniently characterized by a bilinear moment–rotation relationship in the plastic hinges of the beams and columns, described by means of two characteristic points, i.e. the yielding (M_y and θ_y) and ultimate (M_u and θ_u) moment and rotation. The moment M_y can be determined by moment–curvature analyses for the element’s extreme sections. In particular, a mean concrete strength of $f_c = 26.7$ MPa and a steel yield stress of $f_y = 370$ MPa are assumed. The latter corresponds to mean yielding value for smooth type steel Aq50 [15] that, considering an hypothesized construction age of 1960, was one of the most used type of steel. Yielding and ultimate rotations are derived from the ASCE-SEI41 [17] approach, with updated limit values as suggested in ACI 369R-11 [22]. In particular, yielding rotation θ_y is calculated accounting for a reduced effective stiffness, EI_{eff} , with respect to that of the un-cracked gross section [23], while ultimate rotation θ_{CP} is obtained by summing a plastic rotation α to the yielding one, depending on section characteristics.

As noted in [24], the frame members in OpenSees are modeled as an elastic element connected in series with rotational springs at either end, and the stiffness of these components must be modified so that the equivalent stiffness of this assembly is equivalent to the stiffness

of the actual frame member. Following the approach proposed in [24], the rotational springs are made “ n ” times stiffer than the rotational stiffness of the elastic element in order to avoid numerical problems. To ensure the equivalent stiffness of the assembly is equal to the stiffness of the actual frame member, the stiffness of the elastic element must be “ $(n+1)/n$ ” times greater than the stiffness of the actual frame member.

2.2 Modification of plastic hinges for damaged elements in PA

For Nonlinear Time History analyses, the seismic behavior of intact buildings may be studied by performing nonlinear static Pushover Analyses (PA). In the same manner, the seismic behavior of damaged buildings may be studied with PA performed on a suitably modified nonlinear model that conveniently account for damage. In fact, given the local damage level in each of the structural elements caused by a hypothetical main-shock, the moment-rotation relationships describing the plastic hinges of the elements that have entered the plastic range are modified as suggested in [2, 25], and a new PA for the structure in its damaged state may be performed.

The flowchart in Figure 2, referring to framed structures, illustrates the basic steps needed to determine the variation in building behavior from the intact to the different damage states.

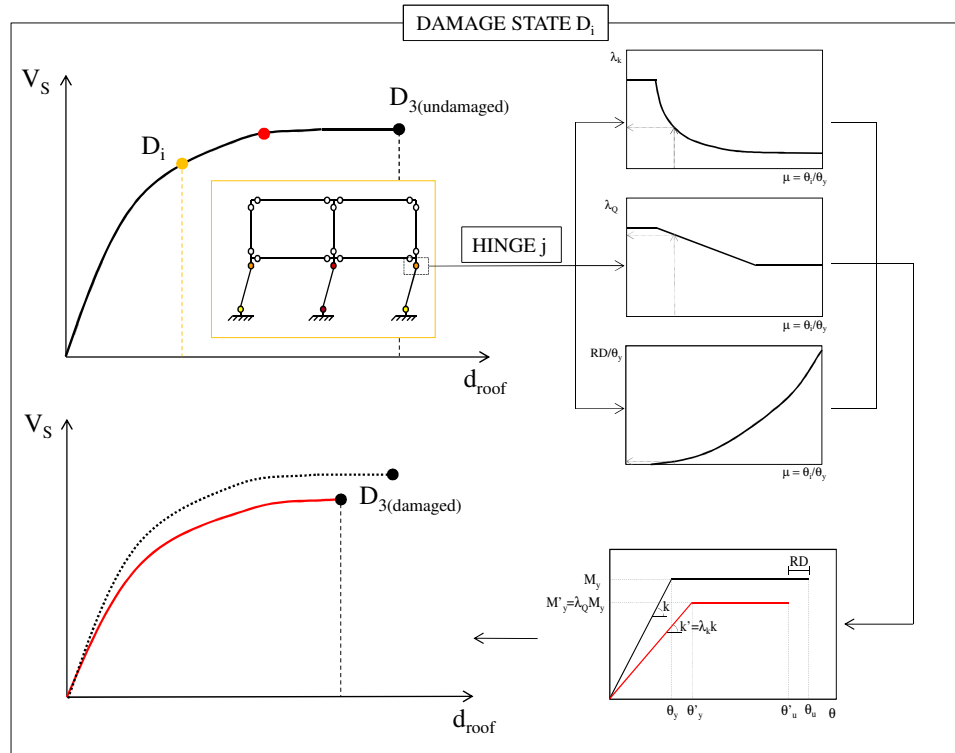


Figure 2: Assessment procedure for a framed structure.

In particular, each global damage level for the structure corresponds to a local distribution of damage for the structural elements, that may be represented by the local ductility demand for the plastic hinges that have entered the plastic range (see left-top panel in Figure 2). Based on the local ductility demand for the elements, the relative plastic hinges are modified (see right panel in Figure 2) applying a suitable variation in the relative stiffness ($K' = \lambda_k K$), strength ($M_y' = \lambda_Q M_y$) and plastic rotation capacity ($a' = a - a_d = a - (\theta_y' - \theta_y) - RD = a - (\theta_y (\lambda_Q / \lambda_k - 1) - RD)$), with λ stiffness or strength modification factors and RD residual drift of the element (for further details see [2, 25]). The PBEE toolbox has been conveniently modified in order to

allow, after computation of the elements ductility demand for the generic step of PA analysis, the modification of plastic hinges with the formulations proposed in [25].

Nonlinear static analysis of the modified damaged models yields pushover curves that, depending on the number of elements involved in the damaged mechanism and on their damage level, may differ significantly with respect to the original ones.

2.3 Modeling issues for Nonlinear Time-History Analysis

The plastic hinges for beam-column elements are modeled with pinching4 material [26] in Opensees [17], that allows to simulate their degrading hysteresis behavior with damage progression. Figure 3 represents the backbone curve of the pinching4 material, evidencing pinched Moment-rotation response and cyclic degradation of strength and stiffness in three ways: unloading stiffness degradation, reloading stiffness degradation, strength degradation. Degradation due to damage is assumed to be a function of displacement history and energy accumulation.

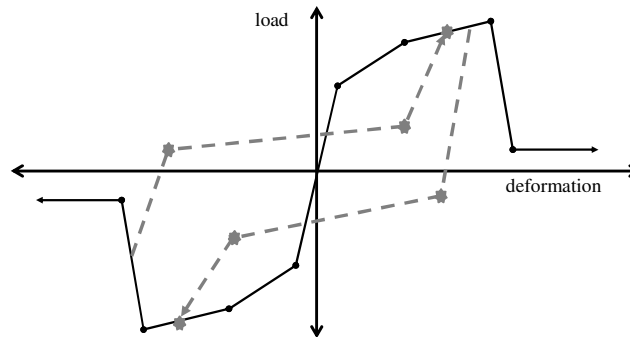


Figure 3: Pinching4 hysteretic material (after [26])

Bilinear backbone has been adopted in order to be consistent with the bilinear model adopted in static PA, furthermore, a slight hardening (0.1% of the Young's modulus) has been considered in plastic phase in order to avoid convergence problems.

For NTH analyses, 5% critical damping was assigned [27]; mass proportional damping was assumed. During the analysis, local P-delta effects were not included.

3 PUSHOVER ANALYSIS FOR INTACT AND DAMAGED BUILDINGS

In order to describe the progression of damage due to a hypothetical mainshock, four global damage states [2] were assumed as reference for the assessment for the case-study buildings:

- D_0 (no damage) in this state the building is still in its intact, or pre-mainshock, condition.
- D_1 (limited damage) corresponds to the onset of non-linear behavior, it is assumed as the Yield Displacement on the Idealized (*YDI*) bilinear pushover curve.
- D_2 (moderate damage) corresponds to the first attainment of the 50% of the Collapse Prevention (*CP*) limit state for an element [2];
- D_3 (collapse) corresponding to the first attainment of the Collapse Prevention limit state (*CP*), that is conventional collapse.

3.1 Analysis of the intact structure

Pushover analysis for the ‘intact’ building was performed applying two different horizontal force distributions (proportional to the main vibration mode MO and proportional to masses MA), as required by modern seismic codes (e.g., [28]). The resulting pushover curves are shown as gray dashed line in Figure 4(a), and 4(b), respectively, referring to 4 and 8 storey RCF under MA forces, and in Figure 4(c) and 4(d) referring to 4 and 8 storey RCF under MO forces, respectively.

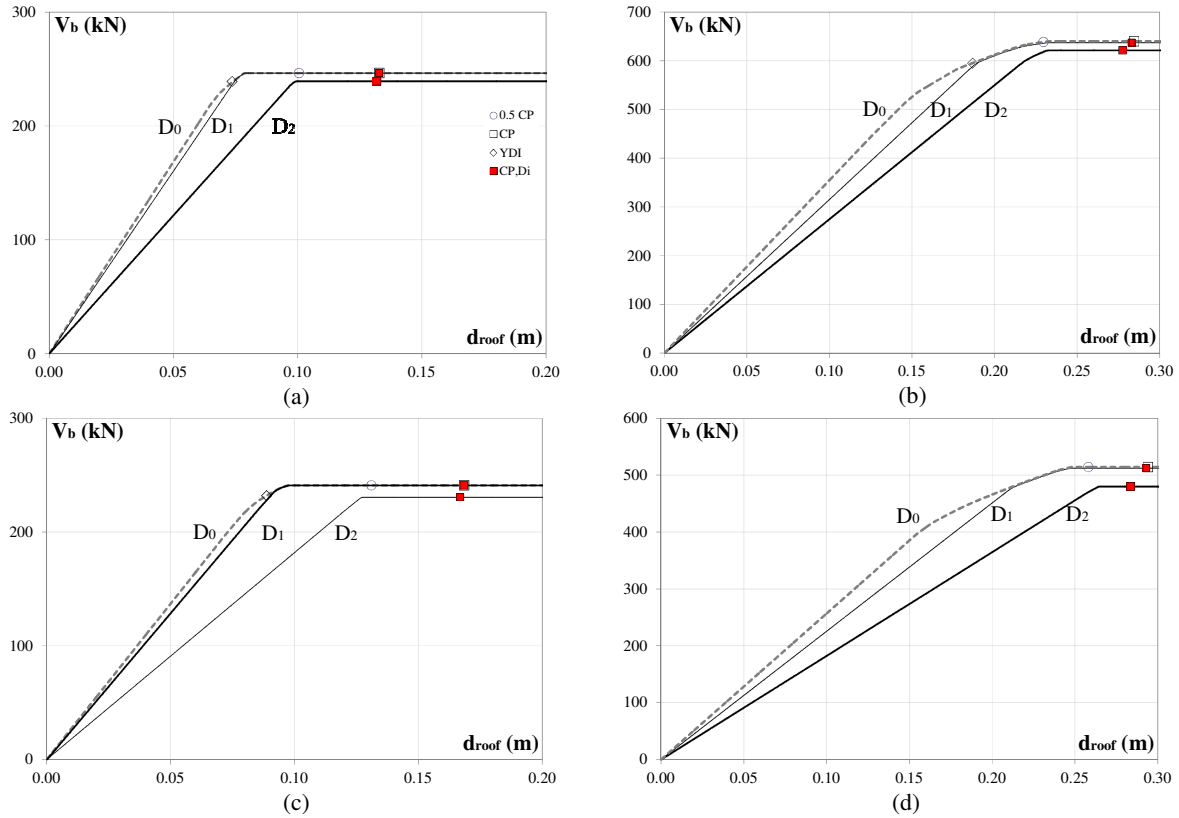


Figure 4: Pushover curves for the 4 and 8 RCFs obtained under MA and MO horizontal forces distribution and for intact (D_0), and D_1 or D_2 damaged states. (a, c) 4 storey MA or MO; (b, d) 8 storey MA or MO

The points marked on the curves in Figure 4, that is, CP , $0.5CP$ and YDI , represent the global damage states D_3 , D_2 , and D_1 that will be considered for further analysis of the ‘damaged’ structure.

The collapse mechanism type for the 4 storey building is the soft storey type at the 1st and 2nd storey, for MA and MO horizontal load distributions, respectively. For the 8 storey building and MA distribution of forces, a two-storey mechanism, involving mainly the columns of the 1st and 2nd storey, is observed, while for 8 storey building with MO a soft-storey mechanism, involving mainly the columns of the 5th level, is formed.

3.2 Analysis of the damaged structure

We study the behavior of the two RCFs for the damage states D_1 and D_2 . For each of the global damage states a separate analysis of the ‘damaged’ structure is performed. Each pushover analysis performed for the “intact” structure is stopped in the deformed configuration at D_k (for $k = 1, 2$) and the plastic hinge state (ductility demand) is recorded. Next, the plastic hinges of the elements that have entered the plastic range are modified as a function of their

ductility demand. Figure 4 shows the pushover curves obtained for each of the considered damaged models. The grey dashed line represent the pushover curves for the intact structure, indicated as D_0 , together with the points corresponding to D_1 and D_2 ; the black thin line represents the Pushover curve obtained for a structure that has attained damage state D_1 and the black bold line for the damage state D_2 . On each of the curves corresponding to the analysis of the damaged building the points corresponding to the first attainment of the (reduced) CP for an element are also shown as small red squares.

The building residual capacity for the intact and damaged states was computed applying the IN2 method [29] on the equivalent SDOF obtained based on the relative PA, as explained in [2]. Tables 1 e 2 summarize the results in terms of REC_{Sa} and REC_{ag} , together with the representative parameters of the equivalent SDOF, obtained after bi-linearization of the capacity curve, T_{eq} , C_b , and μ_{cap} , for the 4 storey and 8 storey building respectively.

ID	Damage	$T_{eq} [s]$	μ_{cap}	$C_b [g]$	$REC_{Sa} [g]$	$REC_{ag} [g]$	PL
MA	D_0	1.42	1.81	0.15	0.26	0.26	0%
	D_1	1.45	1.73	0.15	0.25	0.26	1%
	D_2	1.67	1.34	0.14	0.19	0.19	26%
MO	D_0	1.24	1.89	0.17	0.33	0.27	0%
	D_1	1.47	1.79	0.17	0.31	0.26	2%
	D_2	1.52	1.31	0.17	0.22	0.24	11%

Table 1. Representative parameters of the equivalent SDOF system for the structure in different configurations (intact and damaged) and REC in terms of spectral acceleration and anchoring (peak) ground acceleration, for the 4 storey building

ID	Damage	$T_{eq} [s]$	μ_{cap}	$C_b [g]$	$REC_{Sa} [g]$	$REC_{ag} [g]$	PL
MA	D_0	1.98	1.52	0.19	0.29	0.53	0%
	D_1	2.07	1.39	0.19	0.27	0.52	2%
	D_2	2.21	1.23	0.19	0.23	0.50	5%
MO	D_0	1.68	1.41	0.21	0.30	0.39	0%
	D_1	1.77	1.28	0.27	0.27	0.39	1%
	D_2	1.88	1.15	0.24	0.24	0.38	3%

Table 2. Representative parameters of the equivalent SDOF system for the structure in different configurations (intact and damaged) and REC in terms of spectral acceleration and anchoring (peak) ground acceleration, for the 8 storey building

It is here noted that, in order to allow appropriate comparison with NTH, the spectrum assumed to determine REC_{ag} from REC_{Sa} is the mean spectrum built from the accelerograms in NTH (see § 4.1). The mean spectrum is close to Eurocode 8 [6], soil type B, spectral shape.

Further important information that may be inferred by Table 1 and 2 is the PL for each of the damaged configurations. PL , which represents a measure of the loss of lateral capacity, is defined as:

$$PL = 1 - \frac{REC_{ag,k}}{REC_{ag,0}} \quad (2)$$

where $REC_{ag,k}$ is residual capacity in terms of peak ground acceleration of the structure in the D_k damage configuration and $REC_{ag,0}$ for the intact structure.

4 ASSESSMENT OF DAMAGED BUILDING VIA NTH ANALYSIS

We want to check if the PA, performed on a suitably modified building model accounting for damage experienced during an earthquake, is able to capture the effective variation of building REC and the relative PL .

To this end, the REC_{ag} obtained with the methodology described above, relying on modified building model for two considered damage states, namely D_1 and D_2 , is compared to the REC_{ag} that can be obtained via NTH.

Similarly to the approach adopted in [30], in order to study the behavior of the MDOF system after the attainment of the same damage level D_i , as considered for the PA assessment, multiple earthquake sequences are built through suitable scaling of selected accelerograms. In particular, each nonlinear time history analysis is performed applying sequences of two suitably scaled earthquakes. The first one has to be scaled at the intensity able to “damage” the MDOF system to the same damage level considered on the initial pushover (D_1 or D_2). In order to find this damaging intensity, Incremental Dynamic Analysis (IDA) [31], with the aid of PBEE toolbox [16], is performed and the intensities determining the attainment of D_1 and D_2 and D_3 on the initially intact structures, $a_{g,D1}$, $a_{g,D2}$ and $a_{g,D3}$ are retrieved. In particular, $a_{g,D3}$ and $a_{g,D2}$ correspond to the first attainment on IDA curve of CP and CP/2 rotation for a structural element, and $a_{g,D1}$ corresponds to the identification on IDA curve of the maximum Interstorey Drift Ratio (IDR_{max}) corresponding to the YDI evaluated with PA analysis. $a_{g,D3}$ is, by definition, the REC_{ag} for the intact structure computed based on NTH for a single earthquake.

The second earthquake (applied after the first one scaled at a_{g,D_i}) is the sole one that is successively scaled, performing IDA analysis on a structure that has already attained a given damage state (see Figure 5). This way the $REC_{ag,i}$, varied with respect to the initial one determined on the intact structure, may be determined as the a_g (to which the second accelerogram has to be scaled) corresponding to building collapse (D_3 state, as defined above).

The PBEE has been modified in order to allow scaling only second record in the sequence, while the first record one is scaled to a fixed IM, namely $a_{g,D1}$ or $a_{g,D2}$, that corresponds to the reaching of a given damage state. A time gap of 20 seconds between first earthquake and second earthquake is added between multiple earthquake events (see Figure 5).

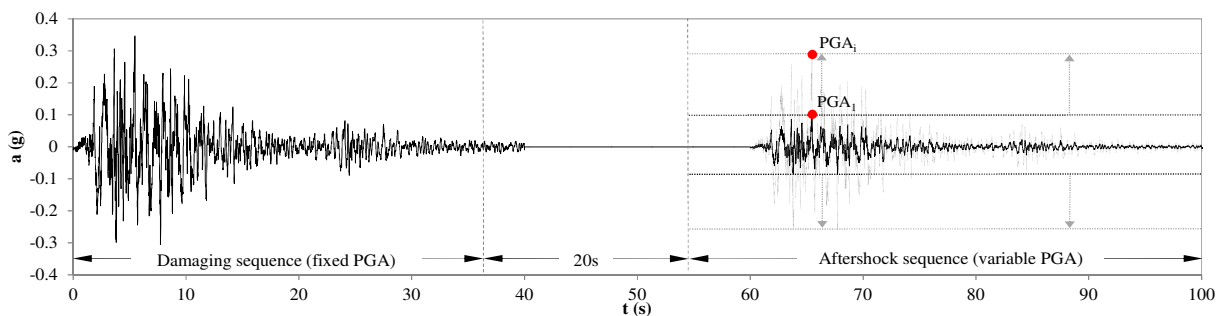


Figure 5: Example seismic sequence.

After the excitation of the first record, the vibration of structure will cease gradually due to damping, so that when the second earthquakes arrives it may be considered as a new one; on the other hand, the structural elements and plastic hinges had been previously damaged by the

first record and this shall be properly accounted for by application of the earthquakes in such a “continuous” sequence.

Dynamic analysis of the sequence is repeated with increasing scale factors applied to the second records in the series until the structure collapses, providing incremental dynamic analysis results for structures having attained a given damage level due to the first earthquake.

For what concerns the NTH evaluation, a set of 8 representative ground motions (16 accelerograms, considering the x and y directions of the recorded signals) is selected in order to be compatible with EC 8 spectrum for Soil Type B (stiff soil) [6]. To account for the effect of record-to-record variability on structural response, IDA is repeated for each of 16 ground motions in the set.

By combining each of the 16 “damaging” ground motions with the same 16 ground motions applied as subsequent earthquakes, a set of 256 record sequences are created for each damage state and structure model.

4.1 Seismic action

A set of 8 couples of response spectrum compatible natural accelerograms has been used to perform Incremental dynamic analyses (see Table 3). Different combinations of first record-second record have been performed in order to simulate damaging earthquake and a subsequent variation in residual capacity in a more realistic way. These records are earthquakes with M_w between 5.4 and 6.9 and sites with epicentral distance 2.9 to 72.0 km. The unscaled records have peak ground accelerations from 0.11 to 0.40 g.

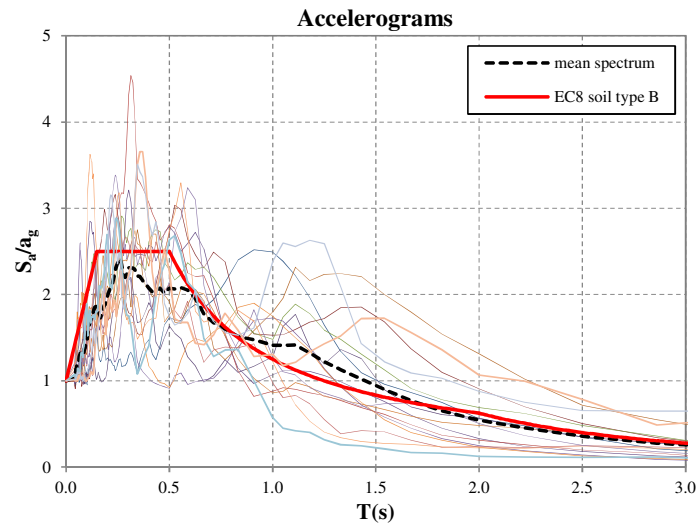


Figure 6: Acceleration spectra for accelerograms recorded on stiff soil.

Single earthquakes were selected from *European Strong-Motion Database* [32], according to the following criteria: a) magnitude of event equal to or greater than 4.0; b) available information about the soil condition, which correspond to Soil Type B [6]; c) seismic sequences having peak ground acceleration (a_g) of the mainshock horizontal component greater than 100 cm/s²; d) significant duration smaller than 35 s; e) Cosenza and Manfredi Index smaller than 12 [33, 34]. Under these criteria 8 seismic earthquakes with two orthogonal horizontal components were selected for this investigation. Table 3 lists the selected earthquakes and significant seismological parameters.

Earthquake Name	Station	Code	M_w	a_g (g)	I_D	Significant duration [35] (s)	Epicentral distance (km)
Montenegro -15/4/1979	Ulcinj-Hotel Olimpic, NS	197x	6.9	0.29	10.6	20.9	24
Montenegro -15/4/1979	Ulcinj-Hotel Olimpic, EW	197y	6.9	0.24	7.2	21.7	24
Montenegro -15/4/1979	Bar-Skupstina Opstine, NS	199x	6.9	0.38	8.4	17.9	16
Montenegro -15/4/1979	Bar-Skupstina Opstine, EW	199y	6.9	0.36	10.4	15.7	16
Kalamata -13/9/1986	D2.7 Kalamata-Prefecture, N265	413x	5.9	0.21	5.4	5.5	5.9
Kalamata -13/9/1986	Kalamata-Prefecture, N355	413y	5.9	0.30	5.8	7.1	5.9
Kalamata -13/9/1986	Kalamata-OTE Building, N80E	414x	5.9	0.24	4.6	5.1	2.9
Kalamata -13/9/1986	Kalamata-OTE Building, N10W	414y	5.9	0.27	7.4	6.3	2.9
Umbria-Marche - 06/10/97	Colfiorito, NS	622x	5.5	0.12	5.2	8.4	5.5
Umbria-Marche - 06/10/97	Colfiorito, EW	622y	5.5	0.11	6.7	7.2	5.5
Filippias - 16/06/90	Vasiliki town-Hall, NS	1981x	5.5	0.14	8.7	12.0	59
Filippias - 16/06/90	Vasiliki town-Hall, EW	1981y	5.5	0.12	10.2	12.0	59
Mt. Hengill Area - 04/06/98	Thorlakshofn, NS	5081x	5.4	0.20	9.3	10.9	21
Mt. Hengill Area - 04/06/98	Thorlakshofn, EW	5081y	5.4	0.37	8.3	10.9	21
Kozani - 13/05/95	Katerini-Agriculture Institute, NS	6101x	6.5	0.40	9.2	32.2	72
Kozani - 13/05/95	Katerini-Agriculture Institute, SW	6101y	6.5	0.34	10.4	32.2	72

Table 3. Accelerograms used in the study

Figure 6 shows the elastic 5% damped spectra for the selected earthquakes as well as their mean acceleration spectrum. The mean spectrum is quite similar and even higher for periods around 1.0 to 2.5s as EC 8 spectrum for Soil Type B [6].

4.2 Study of damaging sequences

As explained in § 4.1, for each record initially applied on the structure the intensity measure (in terms of a_g) corresponding to the attainment of damage level D_i is estimated via IDA.

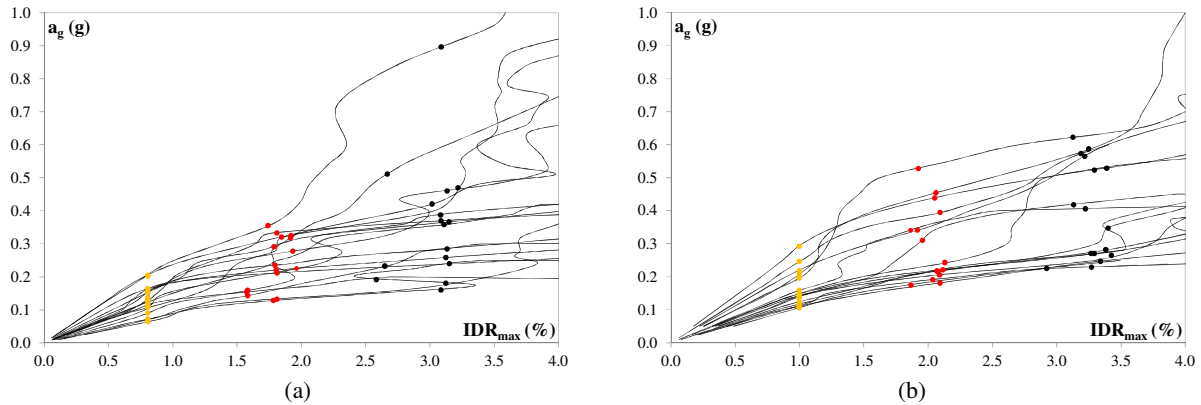


Figure 7: IDA curves for 'intact' buildings subjected to each mainshock. (a) 4 storey, (b) 8 storey building.

In Figure 7 the IDA results for the 4-storey intact building are shown, where x-axis represents the Maximum experienced Inter-storey Drift Ratio (IDR_{max}) and the y-axis the peak ground acceleration (a_g). The dot points marked on each IDA curve, that is, CP (black), $0.5CP$ (red) and that corresponding to the yield displacement of the idealized pushover curve (orange), represent the attainment of global damage states D_3 , D_2 , and D_1 that will be considered for further analysis of the 'damaged' structure, respectively. Due to differences in frequency content, duration and other ground motion characteristics, each ground motion have to be scaled to a different intensity before a particular damage level occurs.

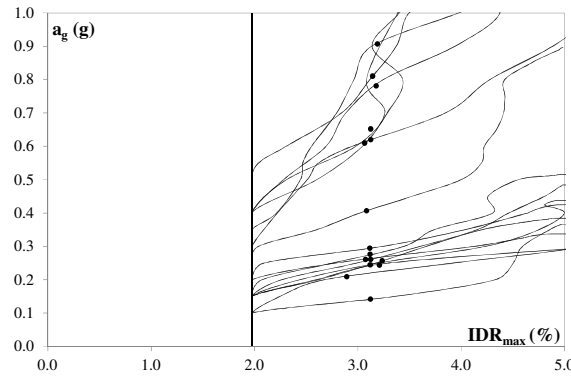


Figure 8: IDA curves for 4 storey building in D_2 , subjected to record 197x

Once the $a_{g,D1}$ (or $a_{g,D2}$) is found for each damaging earthquake (first record), the (first record-second record) sequence may be built; the first record is scaled to $a_{g,D1}$ (or $a_{g,D2}$) while the second record has to be scaled in order to perform IDA on D_1 or (D_2) damaged structure. The results for the 4 storey RCF obtained from those IDA sequences are shown in Figure 8 that refers to the record 197x as (first record) damaging earthquake, scaled to $a_{g,D2} = 0.22$. Each point on those curves represent IDR_{max} (maximum interstorey drift ratio) that is attained in correspondence of each intensity level a_g (of the second ground motion in the sequence). Black dots in Figure represent the MDOF response when $D_3|D_2$ damage state is obtained.

Results are shown for 4-storey building that has reached damage state D_2 due to the first record. The black bold line indicates the threshold after which the interstorey drifts undergone during the second record are greater than those experienced during the first record. Indeed, when applying the earthquake sequence, the IDR_{max} that is registered in each analysis will be always the IDR_{max} corresponding to the first earthquake until the second earthquake has an IM such as to let the maximum inter-storey drift increase. The Figure shows significant scatter in the intensity levels at which a particular damage state occurs for different records after the same damaging (first) record.

5 COMPARISON OF PA AND NTH RESULTS

In this paragraph a comparison between PA and NTH results for the two considered MDOF RCFs is performed. In particular, with the aim of assessing the ability of PA to evaluate the behavior of damaged buildings, we make reference to systems that have attained varying damage levels due to hypothetical main-shocks.

First comparison is performed in terms of the IDR_{max} . Initially, the IDR_{max} distribution along the height for buildings in the undamaged state are compared. In particular, making reference to increasing levels of earthquake demand, i.e. such as to determine the attainment of D_2 or D_3 damage states on the RCFs, the IDR_{max} shapes obtained through pushover analyses with MA or MO forces distribution (indicated as PA-MA and PA-MO, respectively), are compared with the median values (and 16th and 84th fractiles) obtained with the NTH approach. Figure 9 (a, c) shows the diagrams obtained for the initially intact 4 storey RCF at D_2 and at D_3 , respectively. It may be noted, that PA satisfactorily captures the median IDR_{max} shape and value that is obtained through NTH approach; indeed, the plastic mechanism type does not change relevantly for increasing levels of seismic intensity and the MA forces distribution in this case better simulates earthquake response.

Figure 9 (b, d) shows similar diagrams for the 8 storey initially undamaged RCF. Although the storey where maximum IDR_{max} is not suitably identified with PA approach, its value com-

pared with median results obtained with NTH approach is satisfactorily captured by the PA-MO.

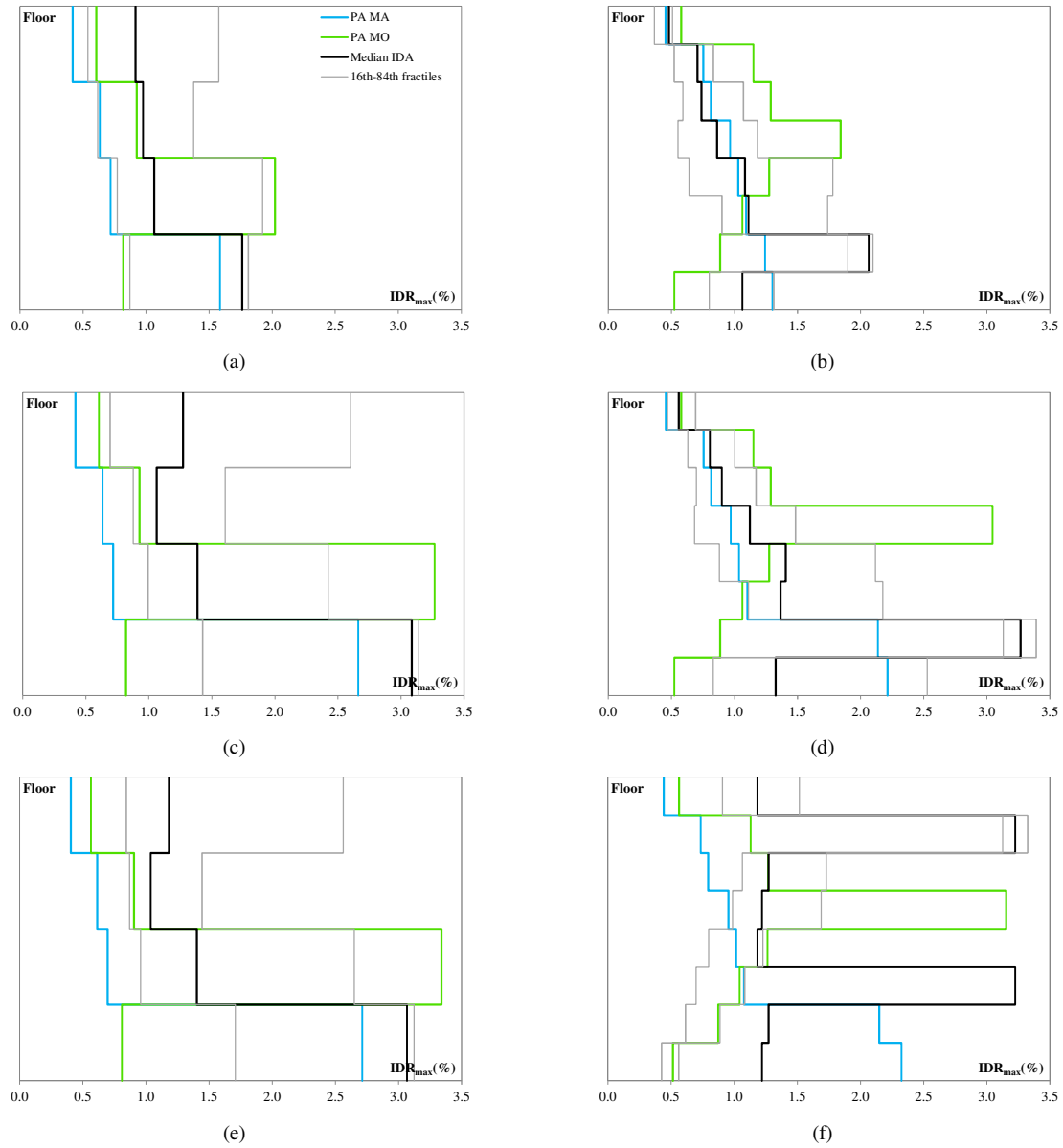


Figure 9: IDR_{max} for 4 storey (a, c, e) and 8 storey building (b, d, f), for ‘intact’ building with respect to D_2 (a, b) and D_3 (c, d), and for D_2 damaged structure with respect to D_3 , i.e. IDR_{max} shape at $D_3|D_2$ (e, f), respectively.

Figure 9 (e, f), referring to 4 and 8 RCFs respectively, show the IDR_{max} distribution along the height at $D_3|D_2$, i.e. derived for systems that had initially sustained D_2 damage state due to the first earthquakes and that arrive at D_3 for the second earthquake (or are pushed to D_3 damage state after modification of the MDOF model for PA analysis).

With reference to the 4 storey RCF (Figure 9 (e)), it can be seen the maximum inter-storey drifts obtained via PA-MA, and the relative distribution, satisfactorily represent the results that may be obtained via NTH analysis approach. Considering the 8 storey RCF (Figure 9 (f)), it is, again, noted that the maximum inter-storey drifts value is captured with reasonable approximation with PA-MO, while the storey where the concentration of damage occurs is the 5th, differently from NTH analysis evidencing a most probable formation of soft storey at level 7. Such discrepancy could be possibly reduced using an adaptive pushover approach.

Second comparison is performed in terms of the REC_{ag} . Figure 10 (a, b, c, d) shows the comparison in terms of $REC_{ag,i}$ for the two considered MDOF systems and two considered damage level. More in detail, Figure 10 (a) refers to the 4 storey RCF, displaying the $REC_{ag,1}$ for the D_1 damaged system. The single $REC_{ag,1}$ values corresponding to each first record (damaging earthquakes) are represented by a number of points aligned along vertical lines (identified by the same ID). Each group of points with the same ID represent the $REC_{ag,1}$ obtained varying the second record in the relative ID sequence (i.e. the sequence with ID record as the first damaging earthquake).

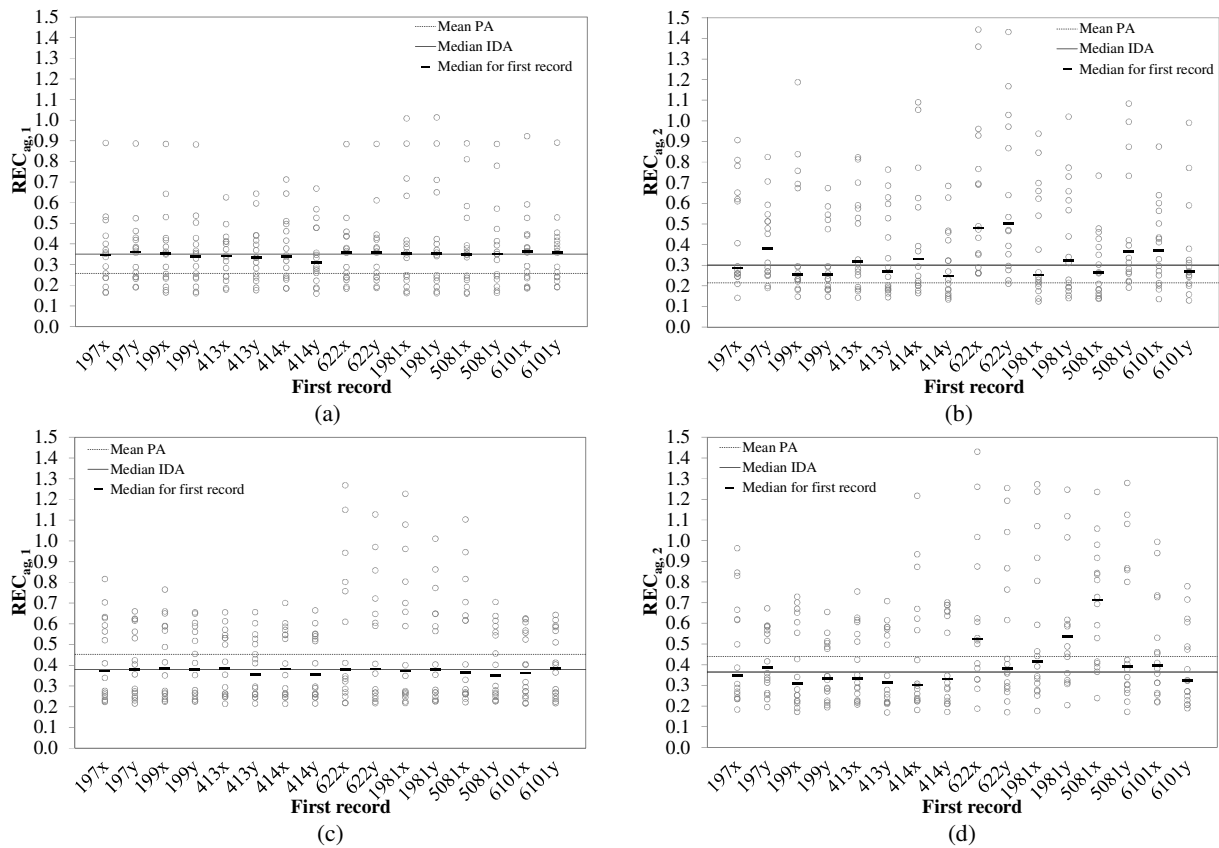


Figure 10: Comparison between PA and NTH computations of $REC_{ag,i}$ for 4 storey (a, c) and 8 storey (b, d) buildings, in damage states D_1 and D_2 respectively.

For each group of first record-second record sequence, the median of $REC_{ag,1}$ is represented by black square, while the horizontal continuous line in figure represents the median obtained as the median of those medians. For comparison, the median value of $REC_{ag,1}$ obtained with PA considering the MO and MA distribution is represented as horizontal dashed line in Figure. Figure 10(b), (c) and (d) show similar results with respect to $REC_{ag,1}$ for the 8 storey RCF, for $REC_{ag,2}$ for the 4 storey RCF and for $REC_{ag,2}$ for the 8 storey RCF.

Observing the Figure 10 a relatively good agreement between the results in terms of $REC_{ag,i}$ obtained with PA, performed on suitably modified model for D_i damaged structure, and those obtained through the consecutive records sequences, suitably scaled as described in § 4, is noted. Table 3 resumes the median $REC_{ag,i}$ that are obtained on the intact structures ($REC_{ag,0}$), as well as those obtained for the structures that had been damaged to D_1 or D_2 damage states ($REC_{ag,1}$ or $REC_{ag,2}$), for both PA and NTH based analyses.

It has to be noted that it may (rarely) happen that, for the single first record-second record sequences, the REC_{ag} computed after the entire sequence is larger than the REC_{ag} computed for the sole first record. This may happen because of different polarity (i.e. direction) of the

second earthquake with respect to the first one; indeed if earthquakes have different polarity the second record may beneficially act in reducing residual displacements attained after the first one. It has been shown [30] that the polarity of second record with respect to first one may impact the post-earthquake fragilities for extensively damaged buildings. This issue was not investigated in the present study and has to be properly taken into account in future works.

It is interesting to observe that median Performance Loss (Eq.(1)) that may be expected considering the results of NTH based analyses, i.e. referring to the ratio of the median $REC_{ag,i}$ versus the median $REC_{ag,0}$, is quite close to the median PL that is computed with pushover based approach. In fact, a PL equal to 3.0% or 17.1% is obtained for 4 storey RCF with NTH based analyses for the D_1 or D_2 damaged structures, while PL equal to 1.4% or 18.5% for the same cases is obtained via pushover based analyses. For the 8 storey RCF, a PL of 1.2% or 4.1% is obtained for PA. Analyzing the D_1 or D_2 damaged structures with the NTH approach a slightly negative PL is found in the former case, probably due to the polarity issue evidenced before, while a PL equal to 3.1% is obtained for the latter case. However, in absolute terms those median PL values retrieved with NTH analysis approach are very close to the PA based results.

	4 storey			8 storey		
	$REC_{ag,0}$	$REC_{ag,1}$	$REC_{ag,2}$	$REC_{ag,0}$	$REC_{ag,1}$	$REC_{ag,2}$
NTH (median (g))	0.36	0.35	0.30	0.38	0.38	0.37
PA (median (g))	0.26	0.26	0.22	0.46	0.45	0.44

Table 4. Comparison between PA and NTH analysis at damage state D_i

6 CONCLUSIONS

The study presented in this paper aims at contributing in the evaluation of the usability of pushover analysis for the assessment of the behavior of damaged buildings.

In particular, the efficiency of Pushover analysis PA to capture the variation of buildings Residual Capacity REC after they have sustained varying damage levels due to hypothetical main-shock is checked by comparison of the PA results with those of Nonlinear Time-History analysis NTH.

Two case study Reinforced Concrete Frames (RCF) are considered, namely a 4 storey and an 8 storey RCFs that have been designed in 1st seismicity class according to old seismic codes in force in the early '60s.

The first PA-NTH comparison is performed for the initially undamaged structures. Concerning the 4 storey building, the PA satisfactorily captures the median IDR_{max} shape and value that is obtained through NTH approach for increasing level of earthquake intensity. For the 8 storey RCF the maximum inter-storey drifts value is captured with reasonable approximation by PA, while the storey where the concentration of damage occurs is not the same as evidenced with NTH approach.

For what concerns the REC_{ag} for the undamaged structure, $REC_{ag,0}$, i.e. the initial residual capacity in terms of a_g , it is noted that PA yields a value that is approximately 30% lower than NTH for the 4 storey building and approximately 20% higher for the 8 storey one.

Next PA-NTH comparison is performed for damaged structures. Concerning IDR_{max} the maximum value and distribution along the height obtained at D_3/D_2 (i.e. at D_3 for structures that were previously damaged to D_2) are, again, well captured for the 4 storey RCF, while for the 8 storey only the maximum value is compliant.

For what concerns the REC variation, it is observed that the same PA-NTH scatter obtained for intact structures is obtained for D_i damaged MDOF (with $i=1, 2$). Indeed, $RE-C_{ag1,PA}/RE-C_{ag1,NTH}$ ratio for the 4 storey building is 0.74 and for the 8 storey one is 1.18, while the $RE-C_{ag2,PA}/RE-C_{ag2,NTH}$ ratio for 4 and 8 storey RCF are 0.73 and 1.19, respectively.

These results suggest that, although applying a pushover based procedure for the assessment of damaged buildings the results will be inevitably affected by a certain degree of approximation with respect to Nonlinear Time History analyses executed on a set of seismic sequences, such approximation does not vary significantly with respect to the one that is obtained with standard Pushover Analyses applied to intact structures.

The study do not pretend to be exhaustive, having compared the results of PA with NTH for only two case study frame building. Moreover, a number of assumptions were applied (e.g. brittle failures and P- Δ effect neglected, varying earthquake polarity not considered).

Further studies will have to address these issues.

ACKNOWLEDGEMENTS

This study was performed in the framework of PE 2010–2013; joint program DPC-Reluis Task 1.1.2: Ordinary and Precast Reinforced Concrete Structures.

REFERENCES

- [1] FEMA. “FEMA 306: Evaluation of earthquake damaged concrete and masonry wall buildings – basic procedures manual”. *Federal Emergency Management Agency*, 1998. Washington D.C
- [2] M. Polese, M. Di Ludovico, A. Prota, G. Manfredi, Damage-dependent vulnerability curves for existing buildings. *Earthquake Engineering and Structural Dynamics*, (in press), DOI: 10.1002/eqe.2249, 2012.
- [3] P. Fajfar, P. Gašperšič, The N2 method for the seismic damage analysis of RC buildings. *Earthquake Engineering and Structural Dynamics*, **25**, 31–46, 1996
- [4] A.M. Mwafy, A.S. Elnashai. Static pushover versus dynamic collapse analysis of RC buildings. *Engineering Structures*, **23**, 407–424, 2001
- [5] P. Bazzurro, C.A. Cornell, C. Menun, M. Motahari, Guidelines for seismic assessment of damaged buildings, Proceeding of the 13thWCEE, Paper No. 1708, Vancouver, Canada, August 1-6, 2004.
- [6] Comité Européen de Normalisation, European Standard EN 1998-1: Eurocode8. Design of structures for earthquake resistance. Part 1. General rules, seismic actions and rules for buildings, Brussels, 2005.
- [7] M. Polese, M. Marcolini, A. Prota, G. Zuccaro, Mechanism based assessment of damaged building's residual capacity. *Computational Methods in Structural Dynamics and Earthquake Engineering, Compdyn 2013*, Paper No. 1524, Kos, Greece, 2013.
- [8] M. Polese, G.M. Verderame, C. Mariniello, I. Iervolino, G. Manfredi, Vulnerability analysis for gravity load designed RC buildings in Naples – Italy, *Journal of Earthquake Engineering*, **12** (S2), 234-245, 2008.

- [9] H. Krawinkler, GDPK. Seneviratna, Pros and cons of a pushover analysis of seismic performance evaluation. *Engineering Structures*, **20**(4-6), 452–64, 1998.
- [10] WK. Tso, AS. Moghadam, Pushover procedure for seismic analysis of buildings. *Progress in Structural Engineering and Materials*, **1**(3), 337–44, 1998.
- [11] RS. Lawson, V. Vance, H. Krawinkler, Nonlinear static push-over analysis — why, when, and how? In: *Proceedings 5th US NCEE*, vol. 1. IL, USA: Chicago; 283–92, 1994.
- [12] S. Antoniou, A. Rovithakis, R. Pinho, Development and verification of a fully adaptive pushover procedure, *12th European Conference on Earthquake Engineering*, paper # 822, London, 2002.
- [13] G. M. Verderame, M. Polese, C. Mariniello, G. Manfredi, A simulated design procedure for the assessment of seismic capacity of existing reinforced concrete buildings, *Advances in Engineering Software*, **41** (2), 323-335, 2010.
- [14] R.D.L. no. 2229/1939. Regulations for the execution of simple and reinforced concrete constructions; 1939 [in Italian].
- [15] G.M. Verderame, P. Ricci, M. Esposito, G. Manfredi, 2012. STIL v1.0 – Software per la caratterizzazione delle proprietà meccaniche degli acciai da c.a. tra il 1950 e il 2000. ReLUIS. <http://www.reluis.it/> (in Italian)
- [16] M. Dolšek, Development of computing environment for the seismic performance assessment of reinforced concrete frames by using simplified nonlinear models. *Bulletin of Earthquake Engineering*, **8**(6), 1309-329, 2010.
- [17] F. McKenna, G.L. Fenves, M.H.Scott, OpenSees: Open system for earthquake engineering simulation, Pacific Earthquake Engineering Research Center, University of California, Berkeley, California, USA, 2004. <http://opensees.berkeley.edu>
- [18] ASCE-SEI 41–06. Seismic Rehabilitation of Existing Buildings, ASCE Standard, American Society of Civil Engineers, Reston, Virginia, 2007.
- [19] G.M. Verderame, M. Polese, E. Cosenza, Vulnerability of existing R.C. buildings under gravity loads: A simplified approach for non sway structures, *Engineering Structures*, **31** (9), 2141-2151, 2009.
- [20] M. Polese, G.M. Verderame, G. Manfredi, Static vulnerability of existing R.C. buildings in Italy: a case study, *Structural Engineering and Mechanics*, Techno-Press, **39** (4), 599-620, 2011.
- [21] C.A. Pagni, L.N. Lowes, Fragility Functions for older reinforced concrete beam-column joints, *Earthquake Spectra*, **22** (1), 215–238, 2006.
- [22] ACI 369R-11. Guide for Seismic Rehabilitation of Existing Concrete Frame Buildings and Commentary. Reported by ACI committee 369, American Concrete Institute, 2011. ISBN: 978-0-87031-419-3
- [23] K.J. Elwood and M.O. Eberhard, Effective stiffness of reinforced concrete columns, *ACI Structural Journal*, **106** (3), 476-484, 2009.
- [24] L.F. Ibarra, H. Krawinkler, Global collapse of frame structures under seismic excitations, Technical Report 152, The John A. Blume Earthquake Engineering Research Center, Department of Civil Engineering, Stanford University, Stanford, CA, 2005.

- [25] M. Di Ludovico, M. Polese, M. Gaetani d'Aragona, A. Prota, G. Manfredi, Modeling of damaged RC columns in nonlinear static analyses: a proposal for plastic hinges modification factors. *Engineering Structures*, **51**, 99–112, 2013.
- [26] L.N. Lowes, M. Nilanjan, A. Altoontash, A beam-column joint model for simulating the earthquake response of reinforced concrete frames, PEER Report 2003/10, Pacific Earthquake Engineering Research Center, University of California, Berkeley, February, 2004.
- [27] F.A. Charney, Unintended consequences of modeling damping in structures, *Journal of Structural Engineering*, **134**(4), 581–592, April 1, 2008.
- [28] Comité Européen de Normalisation, European Standard EN 1998–3: Eurocode8. Design of structures for earthquake resistance. Part 3. Assessment and retrofitting of buildings, Brussels, 2004.
- [29] M. Dolsek, P. Fajfar, IN2- A simple alternative for IDA, 13th World Conference on Earthquake Engineering, Paper No. 3353, Vancouver, B.C., Canada, 2004.
- [30] M. Rahunandan, A.B. Liel, H. Ryu, N. Luco, S.R. Uma, Aftershock fragility curves and tagging assessments for a mainshock-damaged building, Proceeding of the 15th WCEE, Paper No. 1708, Lisboa, Portugal, August 1-6, 2004
- [31] D. Vamvatsikos, A. Cornell, Incremental dynamic analysis. *Earthquake Engng Struct. Dyn.*, **31** (3), 491-514, 2002.
- [32] N. Ambraseys, P. Smit, R. Sigbjornsson, P. Suhadolc, and B. Margaris, Internet-site for european strong-motion data, European Commission, Research-Directorate General, Environment and Climate Programme, 2002.
- [33] E. Cosenza, G. Manfredi, Damage indices and damage measures, *Progress in Structural Engineering and Materials*, **2**(1) 50–59, 2000.
- [34] Cosenza E., Manfredi G., Polese M., A simplified method to include cumulative damage in the seismic response of SDOF systems, *Journal of Engineering Mechanics*, ASCE, **135**(10), 1081-1088, 2009.
- [35] M.D., Trifunac and A.G., Brady, A study on the duration of strong earthquake ground motion. *Bulletin of the Seismological Society of America*, **65**, 581-626, 1975.